

## Self-assembly of a Mixed Valence Copper Triangular Prism and Transformation to Cage Triggered by an External Stimulus

Ya-Liang Lai,<sup>†</sup> Xue-Zhi Wang,<sup>†</sup> Xian-Chao Zhou, Rui-Rong Dai, Xiao-Ping Zhou,<sup>\*</sup> and Dan Li



Cite This: <https://dx.doi.org/10.1021/acs.inorgchem.0c02682>



Read Online

ACCESS |



Metrics & More

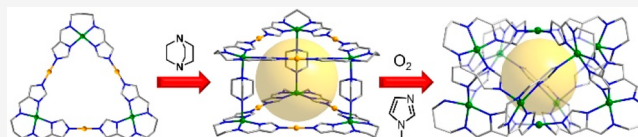


Article Recommendations



Supporting Information

**ABSTRACT:** A triangular prismatic metal–organic cage based on mixed valence copper ions has been designed and synthesized by using metallocycle panels and pillar ligands. The triangular prism will be quickly transformed to a 10-nuclear cage upon an external chemical stimulus, which features a bicapped square antiprism structure. This prismatic cage can act as a catalyst for oxidation of aromatic alcohols to their corresponding aromatic aldehydes with high yields at room temperature under O<sub>2</sub> atmosphere.



### INTRODUCTION

In a biological system, the implementation of functions depends on the robust signal transductions, which usually involve molecular-scale responses to stimuli and conformation changes. To mimic a biological system, chemists investigate the stimuli-responsive behavior at a molecular scale, which will probably help the design of advanced materials that show functions in response to an external stimulus (e.g., light, pH, or the presence of a chemical species).<sup>1</sup> Metal–organic cages (MOCs) containing well-defined cavities via coordination-driven self-assembly are typical models for mimicking enzymes<sup>2</sup> which have a variety of applications, including in separation,<sup>3</sup> recognition and sensing,<sup>3b,4</sup> catalysis,<sup>2,5</sup> and biomedicine.<sup>6</sup> MOCs based on dynamic coordination bonds will probably undergo structural changes after induction of external stimuli, e.g., light,<sup>7</sup> pH,<sup>8</sup> guest,<sup>9</sup> solvents,<sup>10</sup> and crystallization.<sup>11</sup> For example, Clever et al. found that a series of photoactive Pd<sub>2</sub>L<sub>4</sub> coordination cages based on dithienylene-thene ligands allowed triggering of guest uptake and released by irradiation.<sup>7,12</sup> Nitschke et al. reported that the presence of guest ClO<sub>4</sub><sup>−</sup> anions promoted a structural transformation of the M<sub>4</sub>L<sub>6</sub> tetrahedron into an M<sub>10</sub>L<sub>15</sub> pentagonal prism.<sup>13</sup> Crowley et al. designed and synthesized a heterobimetallic PdPtL<sub>4</sub> cage, which can reversibly transform from opened to closed state selectively at one end upon treatment with different stimuli (*N,N'*-dimethylaminopyridine and *p*-toluenesulfonic acid).<sup>14</sup> To the best of our knowledge, however, there are very few MOCs in which both the oxidation states of metal ions and structure are changed after cage-to-cage transformation upon an external stimulus.<sup>15</sup>

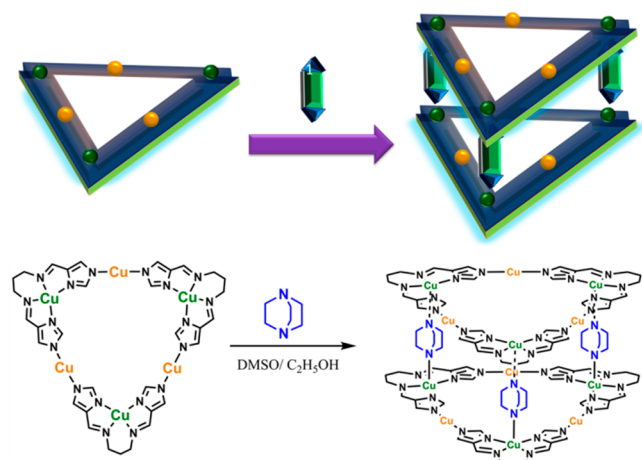
The rational design of coordination cages is available by utilizing the directional feature of coordination bonds and defined coordination geometry of metal ions.<sup>16</sup> Many types of prismatic cages have been successfully designed and synthesized by precisely choosing metal ions and multitopic ligands (e.g., triangular prism,<sup>17</sup> quadrangular prism,<sup>18</sup> pentaprism,<sup>19</sup> and hexagonal prism<sup>20</sup>). The metal–organic triangular prism is

the simplest prismatic structure, which can be obtained by combination of the end-capped metal centers as vertexes, the tritopic planar ligand as roofs and floors, and the bidentate linear ligands as pillars in a 6:2:3 molar ratio.<sup>21</sup> Alternatively, a triangular prism can be obtained by assembly of a two-component approach by using three 0° Pt-based molecular clips to connect two tripodal organic panels.<sup>22</sup> Furthermore, the heteroleptic triangular prism can be synthesized by a three-component reaction of pyridyl and carboxylate ligands with platinum acceptors.<sup>23</sup> Although many metal–organic triangular prisms have been reported,<sup>24</sup> the method of designing a triangular prism by the combination of metal–organic triangular panels and pillar ligands is rarely reported.<sup>25</sup>

In our previous work, we had designed and synthesized a series of hexanuclear mixed valence and heteronuclear triangular metallocycles by using a metalloligand approach.<sup>26</sup> We speculated that we could probably utilize the metallocycles as the triangular panels to construct a triangular prismatic MOC (Scheme 1) based on following reasons. (1) The triangular metallocycle is stable and rigid, and (2) each metallocycle contains three four- or five-coordinated Cu<sup>II</sup> centers with weak coordinated anions, which are possibly coordinated by bidentate pillar ligands to fabricate a triangular prism. In this work, we report the design and assembly of a prismatic MOC formed through coordination of the Cu<sup>II</sup> ions of the metallocycles and bidentate ligands (Scheme 1), formulated as [Cu<sup>I</sup><sub>3</sub>(Cu<sup>II</sup>L1)<sub>3</sub>]<sub>2</sub>L2<sub>3</sub>·8ClO<sub>4</sub>·2H<sub>3</sub>O<sup>+</sup> (denoted as 1, H<sub>2</sub>L1 = *N,N'*-(propane-1,3-diyl)bis(1-(1H-imidazol-4-yl)methanimine) and L2 = triethylenediamine), which features

Received: September 8, 2020

**Scheme 1. Schematic Diagram of Self-assembly of the Mixed Valence Metal–Organic Triangular Prism from Triangular Metalloctetrahedra and Pillar Ligands**



a mixed valence triangular prism structure. The prism **1** is composed of two mixed valence metalocycles and three L2. We found that prism **1** can slowly transform to a metal–organic bicapped square antiprism in organic solvent, which contains ten  $\text{Cu}^{\text{II}}$  and eight L1. Interestingly, the reacting rate can be highly boosted by adding *N*-methylimidazole (NMI) to the reaction mixture, which acts as an organic stimulus for the structure transformation. Furthermore, prism **1** can act as a catalyst for selectively oxidizing the aromatic alcohol to corresponding aldehydes at room temperature.

## RESULTS AND DISCUSSION

Prism **1** was synthesized by the assembly of the metalocycle and pillar ligand L2 with a mole ratio of 2:3 in a mixed solvent (dimethyl sulfoxide DMSO/ethanol, 4:1, v/v) at 80 °C for 6 h (for details see the Supporting Information), which was protected under nitrogen atmosphere. The green crystalline powder mixed with a few single crystals was obtained with a very high yield (98%). In the reaction, the organic ligand L1 was synthesized from condensation of 4-formylimidazole with 1,3-diaminopropane, while the hexanuclear mixed valence metalocycle,  $\text{Cu}_6\text{L1}_3$ , was obtained by using a stepwise synthesis strategy (Scheme S1).<sup>26</sup> Furthermore, the nitrogen protection is critical for synthesis of prism **1**. When the reaction was not protected by  $\text{N}_2$ , prism **1** cannot be successfully obtained, which is probably caused by oxidation of the  $\text{Cu}^{\text{I}}$  centers in  $\text{Cu}_6\text{L1}_3$ . Moreover, we also tested other typical pillar ligands including pyrazine and 4,4'-bipyridine; however, the prismatic metal–organic cage was not successfully obtained. The possible reason is due to that pyrazine and 4,4'-bipyridine are relatively weaker Lewis bases.

Single-crystal X-ray diffraction (SCXRD) analysis revealed that prism **1** crystallizes in a hexagonal  $P6_3/mmc$  space group, which is obviously different from that of  $\text{Cu}_6\text{L1}_3$  ( $P1$ ). As shown in Figure 1, the hexanuclear triangular metalocycle is similar to  $\text{Cu}_6\text{L1}_3$ , which is further pillared by L2 to form the triangular prism **1**. In prism **1**, there are six  $\text{Cu}^{\text{II}}$  and six  $\text{Cu}^{\text{I}}$  centers, six L1, three L2, and eight  $\text{ClO}_4^-$ . The skeleton of **1** is positive (+6), which is charge-balanced by the  $\text{ClO}_4^-$ . However, there are two excess  $\text{ClO}_4^-$  anions in the crystal lattice, which are probably charge-balanced by two hydroniums ( $\text{H}_3\text{O}^+$ ). The  $\text{Cu}^{\text{II}}$  is five-coordinated and adopts a distorted

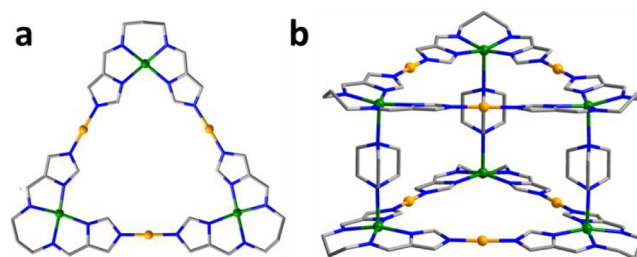


**Figure 1.** Metalloctetrahedron structure in prism **1** (a) and the triangular prismatic cage structure of **1** (b). Color codes:  $\text{Cu}^{\text{II}}$ , green;  $\text{Cu}^{\text{I}}$ , orange; C, light gray; N, blue. All hydrogen atoms and anions are omitted for clarity.

square pyramidal geometry, while the  $\text{Cu}^{\text{I}}$  adopts a linear coordination geometry. The  $\text{Cu}^{\text{II}}\text{--N}$  bond distances are in the range of 1.991–2.297 Å, and the  $\text{Cu}^{\text{I}}\text{--N}$  bond distance is 1.860 Å. The coordination bond distances in prism **1** are in good agreement with those in  $\text{Cu}_6\text{L1}_3$ . The difference between the metalocycle in **1** and  $\text{Cu}_6\text{L1}_3$  is the planarity. The triangular  $\text{Cu}_6\text{L1}_3$  is distorted, while metalocycle of **1** becomes planar after coordination to L2 (Figure S1).

Prism **1** is a regular prism, in which its height is about 7.166 Å and its width of triangle base is about 11.654 Å. Interestingly, similar to  $\text{Cu}_6\text{L1}_3$ , the cavities of the two triangular metalocycles in **1** are occupied by  $\text{ClO}_4^-$  anion as a guest, as shown in Figure 2a. The  $\text{ClO}_4^-$  ions are located in the

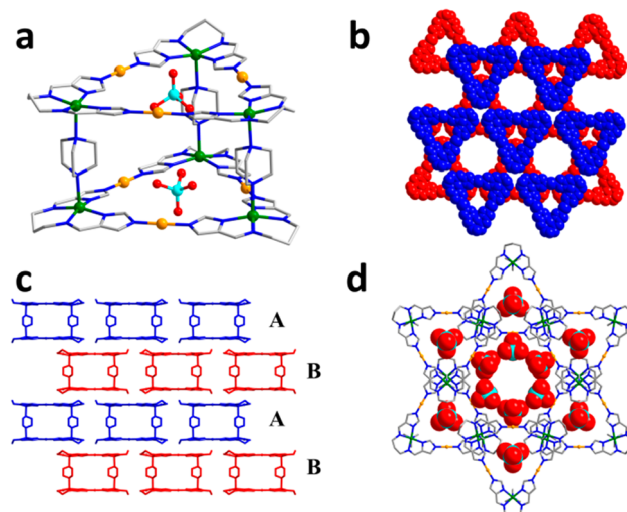


**Figure 2.** Encapsulation of  $\text{ClO}_4^-$  anions by the metalocycles of **1** (a); the “ABAB” packing structure of **1** along the  $c$ -axis (b, space-filling mode), the “ABAB” packing structure of **1** along the  $b$ -axis (c); and a hexagonal channel filled with  $\text{ClO}_4^-$  anions (d). Color codes:  $\text{Cu}^{\text{II}}$ , green;  $\text{Cu}^{\text{I}}$ , orange; C, light gray; N, blue; O, red; Cl, light blue. All hydrogen atoms are omitted for clarity.

center of the metalocycle panels. The encapsulation of  $\text{ClO}_4^-$  ions is probably due to the weak  $\text{C}\cdots\text{H}\cdots\text{O}$  interactions ( $\text{H}\cdots\text{O}$  bond distance of 2.602 Å, Figure S2) and electrostatic effect between  $\text{ClO}_4^-$  and positive skeleton of prism **1**. As shown in Figure 2b and 2c, prism **1** can be described as an “ABAB” layer packing where each prism has six nearest neighbors. Regular hexagonal channels are formed by packing these prisms with a diameter about 12.39 Å (defined by  $\text{H}\cdots\text{H}$  distance of diagonal imidazole groups, without consideration of van der Waals force), which are filled with  $\text{ClO}_4^-$  anions (Figure 2d). The

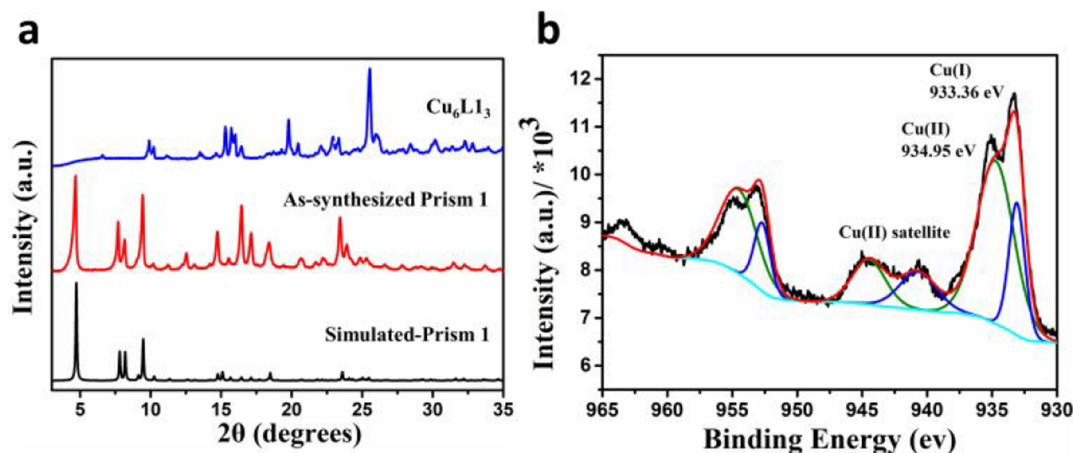


**Figure 3.** PXRD patterns of the as-synthesized metallocycle  $\text{Cu}_6\text{L}_3$  and prism **1** and the calculated pattern from the single-crystal structure of prism **1** (a). XPS spectrum of prism **1** with fitting peaks (b, blue  $\text{Cu}^{\text{I}}$ , green  $\text{Cu}^{\text{II}}$ ).

total potential solvent area volume of **1** is  $3977 \text{ \AA}^3$  (43.5%) in a unit cell, which was checked by the PLATON program.

Powder X-ray diffraction (PXRD) analysis showed that the PXRD pattern of prism **1** closely matched with its simulated patterns from SCXRD data, indicating that the pure phase of prism **1** was obtained (Figure 3a). The PXRD pattern of prism **1** was obviously different to the pattern of  $\text{Cu}_6\text{L}_3$ , indicating the successful assembly of prism **1** from metallocycle and L2. X-ray photoelectron spectroscopy (XPS) is an important tool used to characterize the type and valence state of metal ions. To confirm the oxidation of the copper centers in the prism **1**, the XPS spectrum of prism **1** was measured. As shown in Figure 3b, the spectrum of prism **1** showed a strong asymmetric Cu  $2p_{3/2}$  photoelectron peak with satellite peaks, indicating the mixed valence characteristic of the copper center in prism **1**.<sup>27</sup> The Cu  $2p_{3/2}$  peaks can be deconvoluted into two contributions, which are located at 933.36 and 934.95 eV, respectively (Figure 3b), which is in good agreement with that of metallocycle  $\text{Cu}_6\text{L}_3$ . Bond valence sum (BVS) also has been utilized to determine the oxidation state of copper ions in prism **1**.<sup>28</sup> The calculations of the BVS value for the five-coordinated Cu center gives 2.071, while that for the linear coordination Cu center gives 0.949. The BVS results of prism **1** are consistent with that of metallocycle  $\text{Cu}_6\text{L}_3$ . Both XPS and BVS calculations indicate the mixed valence states of copper centers in prism **1**, which is similar to  $\text{Cu}_6\text{L}_3$ .

Thermogravimetric analysis (TGA) revealed that prism **1** was thermally stable up to approximately  $262 \text{ }^\circ\text{C}$  (Figure S3). To study its porous property,  $\text{N}_2$  adsorption measurement was carried out. The activated **1** could adsorb approximately about  $30 \text{ cm}^3 \text{ g}^{-1} \text{ N}_2$  (77 K,  $P/P_0 = 0.3$ , Figure S4). The Brunauer–Emmett–Teller (BET) and Langmuir surface areas are calculated to be 50 and  $74 \text{ m}^2/\text{g}$ , respectively. The lower  $\text{N}_2$  adsorption for **1** is probably due to the pores of **1** being blocked by the partial decomposition of its packing structure.

The  $\text{Cu}^{\text{I}}$  centers are presented in the prism **1**, which will probably be oxidized to  $\text{Cu}^{\text{II}}$  and induce the structure change. This hypothesis encourages us to study the cage-to-cage transformation property of prism **1**. The solubility of prism **1** is poor in common organic solvents, e.g., DMSO, DMF, and acetonitrile. However, we found that the prism **1** will slowly dissolve in DMF in 3 days, and a green solution was obtained. Slow vapor diffusion of ethyl acetate into this green solution of **1** provided green rod-like crystals suitable for SCXRD analysis.

SCXRD analysis revealed that the new green crystal crystallizes in a  $C2/c$  space group, which features a bicapped square antiprism cage structure. This cage, formulated as  $\text{Cu}_{10}\text{L}_8 \cdot 4\text{ClO}_4$  (denoted **2**), is identical to our previously reported structure (Figure 4), whose conformation depends on the size

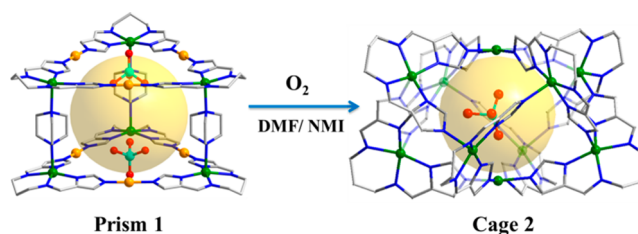


**Figure 4.** Transformation from triangular prism **1** to the bicapped square antiprism **2**.

of anions.<sup>29</sup> Unambiguously, after the transformation, the  $\text{Cu}^{\text{I}}$  center was oxidized to  $\text{Cu}^{\text{II}}$  by  $\text{O}_2$  in the air, and the triangular prism **1** was transformed into **2**. Furthermore, electrospray ionization mass (ESI-MS) spectrometry was employed to study the green solution. As shown in Figure S5, the ESI-MS spectrum showed that the green solution contained **2** and that no **1** was detected, which indicates that the transformation was successful. PXRD analysis showed that the pattern of cage **2** closely matches with its simulated pattern calculated from SCXRD data (Figure S6), suggesting that the product was pure and that prism **1** was completely transformed to cage **2**. We speculated that  $\text{ClO}_4^-$  may play an important role (e.g., as a template) in the transformation process. As shown in Figure 4, after the transformation, one  $\text{ClO}_4^-$  anion was encapsulated in the cavity of cage **2**, which indicates that the  $\text{ClO}_4^-$  anions located in the triangular panels of prism **1** probably templated the formation of cage **2** after the oxidation of  $\text{Cu}^{\text{I}}$  to  $\text{Cu}^{\text{II}}$ .

Although the transformation from prism **1** to cage **2** is successful, the transformation rate is very slow. In biological systems, the conformation change is quick in response to a stimulus. Thus, to mimic a biological system, an accelerated transformation rate is required. In literature, NMI can significantly improve the catalytic effect of lipase<sup>30</sup> and is an important co-catalyst for alcohol oxidation when the copper complexes as the catalyst.<sup>31</sup> Thus, we tried to add NMI into the reaction system to improve the reacting rate for the

transformation. Interestingly, with the addition of NMI (5 equiv of **1**) to the DMF solution, the solid prism **1** dissolved in DMF within about 1 min to give a green solution. The ESI-MS study documented that prism **1** was transformed to cage **2** successfully (Figure S7). The possible reason for NMI accelerating the transformation is due to its strong coordination ability to Cu<sup>I</sup> centers. The binding of NMI on Cu<sup>I</sup> will change its coordination geometry, which probably helps the O<sub>2</sub> oxidation of the Cu<sup>I</sup> centers to Cu<sup>II</sup> and then boosts the transformation process.

In our previous studies, the mixed valence Cu<sup>II</sup>/Cu<sup>I</sup> metallocycle has been a good catalyst for oxidation of (hetero)aromatic alcohols to corresponding (hetero)aromatic aldehydes.<sup>26</sup> Prism **1** also contains the catalytic active Cu<sup>I</sup> sites and has potentially catalytic ability for oxidation of alcohols by employing (2,2,6,6-tetramethylpiperidin-1-yl)oxidanyl (TEMPO) as a co-catalyst and NMI as the base. As shown in Figure S8, prism **1** can catalyze oxidation of 16 (hetero)aromatic alcohols to their corresponding (hetero)aromatic aldehydes with quantitative yields (except 1-naphthalenemethanol 73%) at room temperature under O<sub>2</sub> atmosphere, when the catalyst system consists of 5 mol % **1**, 10 mol % TEMPO, and 50 mol % NMI in acetonitrile. The catalyst system is optimized by following our previous work.<sup>26</sup> Without prism **1** or TEMPO, trace benzyl aldehyde was detected, suggesting that both the prism **1** and TEMPO are indispensable to the oxidation reaction. The scope of this oxidation reaction was found to be very broad, suggesting that prism **1** is a good catalyst. However, the catalytic activity of prism **1** is not good as the metallocycle, which can achieve the same catalytic efficiency under an air condition.<sup>26</sup> Furthermore, prism **1** can also catalyze the sequential alcohol oxidation/Knoevenagel condensation reaction to yield benzylidenemalononitrile (yield 90%) by using benzyl alcohol and malononitrile as starting materials (Scheme S2).

## CONCLUSION

In summary, we have successfully designed and synthesized a mixed valence copper–organic triangular prism by using triangular metallocycle panels and pillar ligands. The copper–organic triangular prism can be transformed to a bicapped square antiprism cage by oxidation of the cuprous ions to cupric ions by air. The NMI molecules can act as a stimulus to accelerate this transformation process. This work provides a new strategy for constructing a metal–organic triangular prism by using a triangular panel and pillar ligand. The NMI boosting the transformation rate provides a unique example for understanding the cage-to-cage transformation.

## ASSOCIATED CONTENT

### Supporting Information

The Supporting Information is available free of charge at <https://pubs.acs.org/doi/10.1021/acs.inorgchem.0c02682>.

Experimental characterizations, additional structural presentations, and FT-IR, PXRD, and ESI-MS analyses (PDF)

### Accession Codes

CCDC 2011494 contains the supplementary crystallographic data for this paper. These data can be obtained free of charge via [www.ccdc.cam.ac.uk/data\\_request/cif](http://www.ccdc.cam.ac.uk/data_request/cif), or by emailing [data\\_request@ccdc.cam.ac.uk](mailto:data_request@ccdc.cam.ac.uk), or by contacting The Cam-

bridge Crystallographic Data Centre, 12 Union Road, Cambridge CB2 1EZ, UK; fax: +44 1223 336033.

## AUTHOR INFORMATION

### Corresponding Author

Xiao-Ping Zhou – College of Chemistry and Materials Science, Guangdong Provincial Key Laboratory of Functional Supramolecular Coordination Materials and Applications, Jinan University, Guangzhou, Guangdong 510632, P. R. China; [orcid.org/0000-0002-0351-7326](https://orcid.org/0000-0002-0351-7326); Email: [zhouxp@jnu.edu.cn](mailto:zhouxp@jnu.edu.cn)

### Authors

Ya-Liang Lai – College of Chemistry and Materials Science, Guangdong Provincial Key Laboratory of Functional Supramolecular Coordination Materials and Applications, Jinan University, Guangzhou, Guangdong 510632, P. R. China

Xue-Zhi Wang – College of Chemistry and Materials Science, Guangdong Provincial Key Laboratory of Functional Supramolecular Coordination Materials and Applications, Jinan University, Guangzhou, Guangdong 510632, P. R. China

Xian-Chao Zhou – College of Chemistry and Materials Science, Guangdong Provincial Key Laboratory of Functional Supramolecular Coordination Materials and Applications, Jinan University, Guangzhou, Guangdong 510632, P. R. China

Rui-Rong Dai – College of Chemistry and Materials Science, Guangdong Provincial Key Laboratory of Functional Supramolecular Coordination Materials and Applications, Jinan University, Guangzhou, Guangdong 510632, P. R. China

Dan Li – College of Chemistry and Materials Science, Guangdong Provincial Key Laboratory of Functional Supramolecular Coordination Materials and Applications, Jinan University, Guangzhou, Guangdong 510632, P. R. China; [orcid.org/0000-0002-4936-4599](https://orcid.org/0000-0002-4936-4599)

Complete contact information is available at:

<https://pubs.acs.org/10.1021/acs.inorgchem.0c02682>

### Author Contributions

<sup>†</sup>These authors contributed equally to this work.

### Notes

The authors declare no competing financial interest.

## ACKNOWLEDGMENTS

This work was supported by the National Natural Science Foundation of China (21731002, 21871172), the Major Program of Guangdong Basic and Applied Research (2019B030302009), the Fundamental Research Funds for the Central Universities (21619405), the Guangzhou Science and Technology Program (202002030411), and Jinan University.

## REFERENCES

- (1) McConnell, A. J.; Wood, C. S.; Neelakandan, P. P.; Nitschke, J. R. Stimuli-Responsive Metal-Ligand Assemblies. *Chem. Rev.* **2015**, *115*, 7729–7793.
- (2) Kaphan, D. M.; Levin, M. D.; Bergman, R. G.; Raymond, K. N.; Toste, F. D. A supramolecular microenvironment strategy for transition metal catalysis. *Science* **2015**, *350*, 1235–1238.

- (3) (a) Xuan, W.; Zhang, M.; Liu, Y.; Chen, Z.; Cui, Y. A Chiral Quadruple-Stranded Helicate Cage for Enantioselective Recognition and Separation. *J. Am. Chem. Soc.* **2012**, *134*, 6904–6907. (b) Zhang, D.; Ronson, T. K.; Lavendomme, R.; Nitschke, J. R. Selective Separation of Polyaromatic Hydrocarbons by Phase Transfer of Coordination Cages. *J. Am. Chem. Soc.* **2019**, *141*, 18949–18953.
- (4) Liu, C.-L.; Zhang, R.-L.; Lin, C.-S.; Zhou, L.-P.; Cai, L.-X.; Kong, J.-T.; Yang, S.-Q.; Han, K.-L.; Sun, Q.-F. Intraligand Charge Transfer Sensitization on Self-Assembled Europium Tetrahedral Cage Leads to Dual-Selective Luminescent Sensing toward Anion and Cation. *J. Am. Chem. Soc.* **2017**, *139*, 12474–12479.
- (5) (a) Cullen, W.; Misuraca, M. C.; Hunter, C. A.; Williams, N. H.; Ward, M. D. Highly efficient catalysis of the Kemp elimination in the cavity of a cubic coordination cage. *Nat. Chem.* **2016**, *8*, 231–236. (b) Jing, X.; He, C.; Yang, Y.; Duan, C. A Metal-Organic Tetrahedron as a Redox Vehicle to Encapsulate Organic Dyes for Photocatalytic Proton Reduction. *J. Am. Chem. Soc.* **2015**, *137*, 3967–3974.
- (6) (a) Sepehrpour, H.; Fu, W.; Sun, Y.; Stang, P. J. Biomedically Relevant Self-Assembled Metallacycles and Metallacages. *J. Am. Chem. Soc.* **2019**, *141*, 14005–14020. (b) Zhao, Y.; Zhang, L.; Li, X.; Shi, Y.; Ding, R.; Teng, M.; Zhang, P.; Cao, C.; Stang, P. J. Self-assembled ruthenium (II) metallacycles and metallacages with imidazole-based ligands and their in vitro anticancer activity. *Proc. Natl. Acad. Sci. U. S. A.* **2019**, *116*, 4090–4098.
- (7) Han, M.; Michel, R.; He, B.; Chen, Y.-S.; Stalke, D.; John, M.; Clever, G. H. Light-Triggered Guest Uptake and Release by a Photochromic Coordination Cage. *Angew. Chem., Int. Ed.* **2013**, *52*, 1319–1323.
- (8) Mal, P.; Schultz, D.; Beyeh, K.; Rissanen, K.; Nitschke, J. R. An Unlockable-Relockable Iron Cage by Subcomponent Self-Assembly. *Angew. Chem., Int. Ed.* **2008**, *47*, 8297–8301.
- (9) Fujita, N.; Biradha, K.; Fujita, M.; Sakamoto, S.; Yamaguchi, K. A Porphyrin Prism: Structural Switching Triggered by Guest Inclusion. *Angew. Chem., Int. Ed.* **2001**, *40*, 1718–1721.
- (10) Zarra, S.; Clegg, J. K.; Nitschke, J. R. Selective Assembly and Disassembly of a Water-Soluble Fe<sub>10</sub>L<sub>15</sub> Prism. *Angew. Chem., Int. Ed.* **2013**, *52*, 4837–4840.
- (11) Stephenson, A.; Argent, S. P.; Riis-Johannessen, T.; Tidmarsh, I. S.; Ward, M. D. Structures and Dynamic Behavior of Large Polyhedral Coordination Cages: An Unusual Cage-to-Cage Interconversion. *J. Am. Chem. Soc.* **2011**, *133*, 858–870.
- (12) (a) Li, R.-J.; Han, M.; Tessarolo, J.; Holstein, J. J.; Lübben, J.; Dittrich, B.; Volkmann, C.; Finze, M.; Jenne, C.; Clever, G. H. Successive Photoswitching and Derivatization Effects in Photochromic Dithienylethene-Based Coordination Cages. *ChemPhotoChem.* **2019**, *3*, 378–383. (b) Li, R.-J.; Holstein, J. J.; Hiller, W. G.; Andréasson, J.; Clever, G. H. Mechanistic Interplay between Light Switching and Guest Binding in Photochromic [Pd<sub>2</sub>Dithienylethene<sub>4</sub>] Coordination Cages. *J. Am. Chem. Soc.* **2019**, *141*, 2097–2103.
- (13) Riddell, I. A.; Smulders, M. M. J.; Clegg, J. K.; Hristova, Y. R.; Breiner, B.; Thoburn, J. D.; Nitschke, J. R. Anion-induced reconstitution of a self-assembling system to express a chloride-binding Co<sub>10</sub>L<sub>15</sub> pentagonal prism. *Nat. Chem.* **2012**, *4*, 751–756.
- (14) Lisboa, L. S.; Findlay, J. A.; Wright, L. J.; Hartinger, C. G.; Crowley, J. D. A Reduced-Symmetry Heterobimetallic [PdPtL<sub>4</sub>]<sup>4+</sup> Cage: Assembly, Guest Binding, and Stimulus-Induced Switching. *Angew. Chem., Int. Ed.* **2020**, *59*, 11101–11107.
- (15) He, Q.-T.; Li, X.-P.; Liu, Y.; Yu, Z.-Q.; Wang, W.; Su, C.-Y. Copper(I) Cuboctahedral Coordination Cages: Host-Guest Dependent Redox Activity. *Angew. Chem., Int. Ed.* **2009**, *48*, 6156–6159.
- (16) Ronson, T. K.; Zarra, S.; Black, S. P.; Nitschke, J. R. Metal-organic container molecules through subcomponent self-assembly. *Chem. Commun.* **2013**, *49*, 2476–2490.
- (17) Zhang, M.; Xu, H.; Wang, M.; Saha, M. L.; Zhou, Z.; Yan, X.; Wang, H.; Li, X.; Huang, F.; She, N.; Stang, P. J. Platinum(II)-Based Convex Trigonal-Prismatic Cages via Coordination-Driven Self-Assembly and C60 Encapsulation. *Inorg. Chem.* **2017**, *56*, 12498–12504.
- (18) (a) Kawano, S.-I.; Fukushima, T.; Tanaka, K. Specific and Oriented Encapsulation of Fullerene C70 into a Supramolecular Double-Decker Cage Composed of Shape-Persistent Macrocycles. *Angew. Chem., Int. Ed.* **2018**, *57*, 14827–14831. (b) García-Simón, C.; Gramage-Doria, R.; Raoufmoghaddam, S.; Parella, T.; Costas, M.; Ribas, X.; Reek, J. N. H. Enantioselective Hydroformylation by a Rh-Catalyst Entrapped in a Supramolecular Metallo cage. *J. Am. Chem. Soc.* **2015**, *137*, 2680–2687.
- (19) Kieffer, M.; Pilgrim, B. S.; Ronson, T. K.; Roberts, D. A.; Aleksanyan, M.; Nitschke, J. R. Perfluorinated Ligands Induce Meridional Metal Stereochemistry to Generate M<sub>8</sub>L<sub>12</sub>, M<sub>10</sub>L<sub>15</sub>, and M<sub>12</sub>L<sub>18</sub> Prisms. *J. Am. Chem. Soc.* **2016**, *138*, 6813–6821.
- (20) (a) Sham, K.-C.; Yiu, S.-M.; Kwong, H.-L. Dodecanuclear Hexagonal-Prismatic M<sub>12</sub>L<sub>18</sub> Coordination Cages by Subcomponent Self-assembly. *Inorg. Chem.* **2013**, *52*, 5648–5650. (b) Nakamura, T.; Kawashima, Y.; Nishibori, E.; Nabeshima, T. Bpytrisalen/Bpytrisaloph: A Triangular Platform That Spatially Arranges Different Multiple Labile Coordination Sites. *Inorg. Chem.* **2019**, *58*, 7863–7872.
- (21) Kumazawa, K.; Biradha, K.; Kusukawa, T.; Okano, T.; Fujita, M. Multicomponent Assembly of a Pyrazine-Pillared Coordination Cage That Selectively Binds Planar Guests by Intercalation. *Angew. Chem., Int. Ed.* **2003**, *42*, 3909–3913.
- (22) Kuehl, C. J.; Yamamoto, T.; Seidel, S. R.; Stang, P. J. Self-Assembly of Molecular Prisms via an Organometallic “Clip. *Org. Lett.* **2002**, *4*, 913–915.
- (23) Zheng, Y.-R.; Zhao, Z.; Wang, M.; Ghosh, K.; Pollock, J. B.; Cook, T. R.; Stang, P. J. A Facile Approach toward Multicomponent Supramolecular Structures: Selective Self-Assembly via Charge Separation. *J. Am. Chem. Soc.* **2010**, *132*, 16873–16882.
- (24) Chakrabarty, R.; Mukherjee, P. S.; Stang, P. J. Supramolecular Coordination: Self-Assembly of Finite Two- and Three-Dimensional Ensembles. *Chem. Rev.* **2011**, *111*, 6810–6918.
- (25) Aoki, S.; Zulkefeli, M.; Shiro, M.; Kimura, E. New supramolecular trigonal prisms from zinc(II)-1,4,7,10-tetraazacyclododecane (cyclen) complexes and trithiocyanurate in aqueous solution. *Proc. Natl. Acad. Sci. U. S. A.* **2002**, *99*, 4894–4899.
- (26) Lai, Y.-L.; Wang, X.-Z.; Dai, R.-R.; Huang, Y.-L.; Zhou, X.-C.; Zhou, X.-P.; Li, D. Self-assembly of mixed-valence and heterometallic metallocycles: efficient catalysts for the oxidation of alcohols to aldehydes in ambient air. *Dalton Trans.* **2020**, *49*, 7304–7308.
- (27) (a) Frost, D. C.; Ishitani, A.; McDowell, C. A. X-ray photoelectron spectroscopy of copper compounds. *Mol. Phys.* **1972**, *24*, 861–877. (b) Zhang, S.; Zhao, L. A merged copper(I/II) cluster isolated from Glaser coupling. *Nat. Commun.* **2019**, *10*, 4848.
- (28) Thorp, H. H. Bond valence sum analysis of metal-ligand bond lengths in metalloenzymes and model complexes. *Inorg. Chem.* **1992**, *31*, 1585–1588.
- (29) Wang, X.-Z.; Sun, M.-Y.; Zheng, J.; Luo, D.; Qi, L.; Zhou, X.-P.; Li, D. Coordination-driven self-assembly of M<sub>10</sub>L<sub>8</sub> metal-organic bi-capped square antiprisms with adaptable cavities. *Dalton Trans.* **2019**, *48*, 17713–17717.
- (30) Liu, B.-K.; Wu, Q.; Xu, J.-M.; Lin, X.-F. N-Methylimidazole significantly improves lipase-catalysed acylation of ribavirin. *Chem. Commun.* **2007**, 295–297.
- (31) (a) Hoover, J. M.; Steves, J. E.; Stahl, S. S. Copper(I)/TEMPO-catalyzed aerobic oxidation of primary alcohols to aldehydes with ambient air. *Nat. Protoc.* **2012**, *7*, 1161–1166. (b) Ryland, B. L.; McCann, S. D.; Brunold, T. C.; Stahl, S. S. Mechanism of Alcohol Oxidation Mediated by Copper(II) and Nitroxyl Radicals. *J. Am. Chem. Soc.* **2014**, *136*, 12166–12173.